Some mathematical properties of the uniformly sampled quadratic phase function and associated issues in digital Fresnel diffraction simulations

Levent Onural
Bilkent University
Electrical and Electronics Engineering Department
TR-06533 Ankara
Turkey
E-mail: onural@ee.bilkent.edu.tr

Abstract. The quadratic phase function is fundamental in describing and computing wave-propagation-related phenomena under the Fresnel approximation; it is also frequently used in many signal processing algorithms. This function has interesting properties and Fourier transform relations. For example, the Fourier transform of the sampled chirp is also a sampled chirp for some sampling rates. These properties are essential in interpreting the aliasing and its effects as a consequence of sampling of the quadratic phase function, and lead to interesting and efficient algorithms to simulate Fresnel diffraction. For example, it is possible to construct discrete Fourier transform (DFT)-based algorithms to compute exact continuous Fresnel diffraction patterns of continuous, not necessarily bandlimited, periodic masks at some specific distances. [DOI: 10.1117/1.1802232]

Subject terms: Fresnel diffraction; quadratic phase function; chirp; diffraction simulation; digital holography; sampling; computer-generated holography; discretization.

Paper 0431110 received Dec. 1, 2003; revised manuscript received Apr. 21, 2004; accepted for publication Apr. 28, 2004.

1 Introduction

Conducting digital simulations of diffraction-related optical phenomena has been a common practice in various applications; computer-generated holography, analysis of holograms by digital means, and the design of diffractive optical elements are a few examples. The Fresnel approximation to diffraction (Ref. 1, Ch. 4) is valid for many practical cases. Therefore, digital simulation of the Fresnel diffraction plays an important role in optics.

The quadratic phase function, $h_\alpha(x,y)=\exp[j\alpha(x^2+y^2)]$, $-\infty<x,\ y<\infty$ is fundamental in optics and other wave-related fields since this function is the kernel of the convolution which represents scalar wave propagation under Fresnel approximation.[1–3] It is also called the 2-D two-sided chirp function, zone lens term, or the Fresnel kernel. This kernel plays an essential role not only in the description of various optical systems, but also in signal processing; for example, the fractional Fourier transform is a form of chirp transform.[4,5]

Discretization of the Fresnel kernel is unavoidable when the Fresnel diffraction is going to be simulated by digital means. Furthermore, discretization naturally occurs when the light interacts with structures that inherently sample the diffraction field, such as gratings with periodic transparent holes over opaque substrates or sensor arrays in imaging devices. Hybrid systems that consist of both analog optical parts and digital processing units employ explicit or implicit sampling of the kernel (or related) functions at some stage of their operations as long as the underlying Fresnel approximation is valid. Sampling and discretization mean exactly the same process within the scope of this paper: a continuous function is represented by a set of numbers corresponding to its values at predefined isolated points.

For example, quadratic phase functions are sampled in Ref. 3 for digital decoding of optically recorded holograms where the diffraction is modeled as a 2-D linear shift invariant system. A similar approach and associated sampling issues are the main topic in Ref. 6. Sampling issues are fundamentally important for the general fast numerical algorithms discussed in Ref. 5. Sampling and the Nyquist rate issues are essential for the digital Fresnel diffraction simulations carried out in Refs. 7 and 8. Numerical reconstruction of holograms at tilted angles involves sampling issues in conjunction with Fresnel approximation in Ref. 9. Computer-generated holographic optical elements such as diffractive grids can also be analyzed within the context of sampling of the diffraction field; interestingly, the processing is not digital but analog in these cases.[10] Recording of holographic signals using CCD arrays (or other discrete recording techniques) essentially involves sampling of holograms; it is shown in Ref. 11 that the full reconstruction is feasible even if the high frequencies of the associated kernel (the two-sided chirp) are severely undersampled. Digital computation of the fractional Fourier transform is also directly related to the sampling of the quadratic phase function.[12] Sampling issues play a primary role in digital reconstructions of the particle field and other types of holograms.[13–15]

Understanding of the properties of the underlying Fresnel kernel under sampling is essential both for correct

interpretation of the sampling results and for designing efficient and correct simulation algorithms. There is no doubt that the sampling-related issues regarding general convolution are well known. Therefore, general convolution with an arbitrary convolution kernel, and the associated discretization, is not the main concern of this paper. Instead, this paper shows that when the convolution kernel is restricted to be the quadratic phase function, then there are implications and benefits reaching far beyond the general case.

There seems to be a widespread tendency to associate bandlimitedness and sampling in almost every problem. Surely, lossless discretization of a continuous function requires some constraints on the set of functions being considered. Bandlimitedness is a common constraint and fits well in many practical cases; and the associated sinc interpolation has been well known since Shannon. What is disturbing is the automatic application of the bandlimitedness constraint to almost any problem, even if there are more obvious and maybe stronger constraints that would lead to much more efficient discretization. Even more disturbing is to give up lossless sampling when the functions do not happen to be bandlimited even if there are much more convenient constraints that would lead to lossless sampling. This tendency is so strong that many even had the wrong impression that lossless sampling is impossible when the functions are not bandlimited! One trivial counterexample is the set of piecewise constant functions (a very strong constraint), $f(t)=c_i$, $iT \leqslant t < (i+1)T$, where T is a constant, and the is are integers. Obviously, these functions are not bandlimited due to step jumps at each iT, but they can be fully recovered trivially from samples taken at instants $\tau + iT$, $0 \leqslant \tau < T$. Of course, the reconstruction (interpolation) method depends on the constraint imposed on the functions, and it is not the sinc interpolator if the constraint is not bandlimitedness.

If the impulse response of a continuous linear shift-invariant system is not an arbitrary function but is restricted to be the quadratic phase function, as in the Fresnel diffraction case, then there is no need for bandlimitedness for full recovery of the input (objects) from samples of the system output[8] (the diffraction field). When the convolution kernel is the quadratic phase function, the Nyquist rate requirement can be easily violated and full recovery may still be possible under other constraints. This observation may yield much more sparse sampling than the Nyquist rate and yields much more efficient digital signal processing. However, the strong tendency to associate sampling always with bandlimitedness has apparently kept many researchers away from this possibility. For example, the bandlimitedness assumption (or externally imposed bandlimitedness by explicit filtering) is unnecessarily used in Ref. 1, pp. 352–354 and Refs. 5 to 7; if the fact that the convolution kernel is a quadratic phase function is used as a constraint instead, significant savings in sampling rate requirements would have been achieved.

These seemingly unusual, but actually not so surprising, observations and the associated efficiency trigger even further interest in sampling properties of the quadratic phase function. Indeed, quadratic phase functions have interesting properties under sampling. The purpose of this paper is to derive and collate some useful relations associated with sampling of the quadratic phase function. The issues related to sampling of the continuous Fresnel hologram to reconstruct the underlying objects digitally are given in Ref. 8. The primary concern here in this paper is different from that in Ref. 8 in the sense that now we concentrate on the sampling of the Fresnel kernel itself and issues related to digital simulations of the Fresnel diffraction. We start from simple and well-known properties of the quadratic phase function, for the sake of completeness, and then we use these basic features to reveal other properties. Then we use these properties to clearly and fully interpret the digital simulations of the Fresnel diffraction using the discrete Fourier transform (DFT).

2 Properties

For notational clarity and simplicity, we start with 1-D signals for the preliminaries; extensions to higher dimensions follows. The 1-D two-sided quadratic phase function is $h_\alpha(x)=\exp(j\alpha x^2)$, $-\infty<x<\infty$. This function is neither space nor band limited; it is not causal, either.

Many properties of the quadratic phase function are well known. A few simple examples, well known in the literature, are briefly repeated here; the intention is to provide continuity as more obscure, but useful, properties are proven later. For example, its Fourier transform is

$$\begin{aligned}\mathcal{F}[h_\alpha(x)] &= \mathcal{F}[\exp(j\alpha x^2)] \\ &= \int_{-\infty}^{\infty} h_\alpha(x)\exp(-j\omega x)\,dx = H_\alpha(\omega) \\ &= \left(j\frac{\pi}{\alpha}\right)^{1/2}\exp\left(-j\frac{\omega^2}{4\alpha}\right). \end{aligned} \tag{1}$$

When $\alpha=1/2$, the Fourier transform of quadratic phase function is equal to a constant times its own complex conjugate. Even though the quadratic phase function is not the eigenfunction of the Fourier transform, in the formal sense, it can still be used in many applications where benefits are expected from using the eigenfunction approach where the conjugation may not be the primary concern.

Other properties of quadratic phase function are also well known. For example, modulation of this function is essentially equivalent to shifting it since $\exp(j\alpha x^2)\exp(j\omega_0 x)=c_{\alpha,\omega_0}\exp[j\alpha(x+\omega_0/2\alpha)^2]$, where $c_{\alpha,\omega_0}=\exp(-j\omega_0^2/4\alpha)$, which is a constant for given ω_0 and α. As a consequence of Fourier transform properties, we get,

$$\begin{aligned}\mathcal{F}[h_\alpha(x)\exp(j\omega_0 x)] &= H_\alpha(\omega-\omega_0) \\ &= c_{\alpha,\omega_0}H_\alpha(\omega)\exp\left(j\frac{\omega_0}{2\alpha}\omega\right). \end{aligned} \tag{2}$$

Therefore, modulation of the quadratic phase function in space domain also results in a modulation in the Fourier domain. Furthermore, when $\alpha=1/2$, $\mathcal{F}[h_{1/2}(x)\exp(j\omega_0 x)] = c_{1/2,\omega_0}H_{1/2}(\omega)\exp(j\omega_0\omega)$. In other words, the modulation of this quadratic phase by a complex exponential function results in the same modulation of its Fourier transform in

the Fourier domain within a constant gain. Having the mentioned modulation/shift equivalence, one can prove that

$$\mathcal{F}[h_\alpha(x+x_0)]=c^*_{1/4\alpha,x_0}H_\alpha(\omega-2\alpha x_0). \tag{3}$$

Thus, shifting a quadratic phase in space also results in a shift of its Fourier transform. This property reduces to $\mathcal{F}[h_{1/2}(x+x_0)]=c^*_{1/2,x_0}H_{1/2}(\omega-x_0)$, when $\alpha=1/2$.

Actually, bearing in mind that $h_\alpha(x)=\exp(j\alpha x^2)$, one can easily show that properties given by Eqs. (2) and (3) are equivalent: starting with Eq. (2), observing that $h_\alpha(x)\exp(j\omega_0 x)=c_{\alpha,\omega_0}h_\alpha(x+\omega_0/2\alpha)$, and substituting x_0 for $\omega_0/2\alpha$, one would get the property given by Eq. (3).

Two simple properties given by Eq. (2) and (3) can be used to construct a rather more obscure one, related to sampling. The sampling property of the Fourier transform states that,

$$\mathcal{F}\left[f(x)\sum_n \delta(x-nX)\right]=\frac{1}{X}\sum_n F\left(\omega-\frac{2\pi}{X}n\right), \tag{4}$$

where X is the sampling period, and $F(\omega)$ is the Fourier transform of $f(x)$. Applying this property to the quadratic phase function and using Eq. (2), we get

$$\begin{aligned}\mathcal{F}\left[h_\alpha(x)\sum_n \delta(x-nX)\right]&=\frac{1}{X}\sum_n H_\alpha\left(\omega-\frac{2\pi}{X}n\right)\\&=\frac{1}{X}\sum_n\left(j\frac{\pi}{\alpha}\right)^{1/2}\\&\quad\times\exp\left[-j\frac{\left(\omega-\frac{2\pi}{X}n\right)^2}{4\alpha}\right]\\&=\frac{1}{X}\sum_n c_{\alpha,2\pi n/X}H_\alpha(\omega)\\&\quad\times\exp\left(j\frac{\pi n}{\alpha X}\omega\right).\end{aligned} \tag{5}$$

Therefore,

$$\begin{aligned}h_\alpha(x)\sum_n \delta(x-nX)=\mathcal{F}^{-1}\Bigg[&\frac{1}{X}\sum_n c_{\alpha,2\pi n/X}H_\alpha(\omega)\\&\times\exp\left(j\frac{\pi n}{\alpha X}\omega\right)\Bigg].\end{aligned} \tag{6}$$

Now, using the well-known property $\mathcal{F}^{-1}[\exp(j\omega x_0)F(\omega)]=f(x+x_0)$, we can rewrite the last equation as

$$h_\alpha(x)\sum_n \delta(x-nX)=\frac{1}{X}\sum_n c_{\alpha,2\pi n/X}h_\alpha\left(x+\frac{\pi}{\alpha X}n\right). \tag{7}$$

This is an important (and not quite obvious) property, which states that the sampled quadratic phase function [the left-hand side of Eq. (7)] is equal to a weighted sum of the shifted versions of the same (original continuous) quadratic phase function. This property is valid for an X and α. Sampling causes severe aliasing since $h_\alpha(x)$ is not bandlimited, but the equation is still valid. The same property may also be interpreted as

$$\begin{aligned}h_\alpha(x)\sum_n \delta(x-nX)=\Bigg[&\sum_n\left(\frac{1}{X}c_{\alpha,2\pi n/X}\right)\\&\times\delta\left(x+\frac{\pi}{\alpha X}n\right)\Bigg]*h_\alpha(x),\end{aligned} \tag{8}$$

where $*$ denotes the convolution operation. Since the coefficients, $c_{\alpha,2\pi n/X}$, are symmetric with respect to n, the impulse train on the right-hand side of Eq. (8) can be replaced by $\delta[x-(\pi/\alpha X)n]$ if desired.

The implication of the form given in Eq. (8) is the key in the interpretation of the effects of using the discrete form of the convolution kernel in wave-propagation related digital simulations, like in computation of diffraction fields, or holograms and their reconstructions[3,8] employing the Fresnel approximation. For example, if the goal is to simulate $f(x)*h_\alpha(x)$, and if the discretized version of $h_\alpha(x)$ is used in simulations, as in many diffraction-related simulation applications, we get,

$$\begin{aligned}f(x)*&\left[h_\alpha(x)\sum_n \delta(x-nX)\right]\\&=f(x)*\left[\sum_n\left(\frac{1}{X}c_{\alpha,2\pi n/X}\right)\delta\left(x+\frac{\pi}{\alpha X}n\right)\right]*h_\alpha(x)\\&=\left[\sum_n\left(\frac{1}{X}c_{\alpha,2\pi n/X}\right)f\left(x+\frac{\pi}{\alpha X}n\right)\right]*h_\alpha(x).\end{aligned} \tag{9}$$

Left-hand side of this equation represents the convolution of a function (input) by the sampled Fresnel kernel. The right-hand side represents the convolution of a function (given in the square brackets) by the continuous Fresnel kernel. Therefore, the effect of discretization of the quadratic phase function is equivalent to replacing $f(x)$ by $\{\Sigma_n[(1/X)c_{\alpha,2\pi n/X}]\ f[x+(\pi/\alpha X)n]\}$ in the original continuous convolution. Since the coefficients, $c_{\alpha,2\pi n/X}$, are just weights, what we have is a convolution of a sum of weighted shifts of original continuous $f(x)$ with the kernel $h_\alpha(x)$. In other words, even though we no longer use the original continuous Fresnel kernel, but its discrete version, we still achieve a result that is equal to the continuous Fresnel diffraction of a function, which is no longer equal to original $f(x)$, but another continuous function closely related to it (weighted periodic replicas). This result has important implications; one example can be found in Ref. 8, where it is shown that exact recovery of objects from their sampled diffraction patterns is still possible even if there is severe aliasing during sampling. By the way, it is well known that a grid (sampling) generates diffraction orders,[10] and actually what is implied by Eq. (9) is equivalent to this fact. Note that the function $f(x)$ is arbitrary in these formulations. It may represent a continuous function, and in this case, the ongoing discussions are for the sake of understanding the issues related to sampling of the qua-

dratic phase function. Or, $f(x)$ may represent the multiplied version of a continuous function by an impulse train and thus the discussion evolves more closer to purely digital simulations; sampling issues of $f(x)$ should also be carefully evaluated as usual. In any case, the discussions related to Eq. (9) are valid for any $f(x)$.

One can relate the sampling period X to α to get specific results. For example, it is possible to have $c_{\alpha,2\pi n/X}=1$ for all n, by choosing $X=(\pi/2\alpha r)^{1/2}$, where r is a positive integer. Such a sampling rate reduces Eq. (7) to,

$$h_\alpha(x)\sum_n \delta(x-nX)=\frac{1}{X}\sum_n h_\alpha\left(x+\frac{\pi}{\alpha X}n\right). \tag{10}$$

Knowing the Fourier transform relation,

$$\sum_n f(x+nP)=\mathcal{F}^{-1}\left[F(\omega)\frac{2\pi}{P}\sum_n \delta\left(\omega-\frac{2\pi}{P}n\right)\right], \tag{11}$$

one can take the Fourier transform of Eq. (10) to get,

$$\mathcal{F}\left[h_\alpha(x)\sum_n \delta(x-nX)\right]=2\alpha H_\alpha(\omega)\sum_n \delta(\omega-2\alpha Xn). \tag{12}$$

This is an interesting result, too: the Fourier transform of sampled quadratic phase function is also equal to a sampled (conjugate) quadratic phase function. If $\alpha=1/2$, and if $X=(\pi/2\alpha r)^{1/2}$, then the Fourier transform of sampled quadratic phase is equal to a constant times its own complex conjugate. Furthermore, the impulsive nature of the Fourier transform (right-hand side) in Eq. (12) implies that $h_\alpha(x)\Sigma_n\delta(x-nX)$ is periodic, and this is also clearly seen from equation (10), where the period is $(\pi/\alpha X)=(2\pi r/\alpha)^{1/2}$. Therefore, even though $h_\alpha(x)$ is not periodic, its sampled version is, if $X=(\pi/2\alpha r)^{1/2}$. This can also be proven directly since,

$$\begin{aligned} h_{\alpha D}[n]\triangleq h_\alpha(nX)&=\exp[j\alpha(nX)^2]=\exp\{j\alpha[(n+Nq)X]^2\}\\ &=h_\alpha(nX+NqX)=h_{\alpha D}[n+Nq]\quad \forall n,q, \end{aligned} \tag{13}$$

for $X=(\pi/2\alpha r)^{1/2}$, and $N=2rp$, where p and q are nonnegative integers.

Finally, the impulsive and periodic nature of both sides of Eq. (12) indicates the N-point DFT relationship for the sampled quadratic phase function. Since $h_{\alpha D}[n]=h_\alpha(nX)$ and $H_{\alpha D}[k]=H_\alpha(2\alpha kX)$, for $n,k\in[0,N-1]$, and if the sampling period is chosen to satisfy $X=(\pi/2\alpha r)^{1/2}$ for a positive integer r, and if $N=2r$, then

$$\begin{aligned} \mathrm{DFT}_N[h_{\alpha D}[n]]&=\sum_{n=0}^{N-1} H_{\alpha D}[n]\exp\left(-j\frac{2\pi}{N}kn\right)\\ &=\frac{1}{X}H_{\alpha D}[k]=\sqrt{jN}h^*_{\alpha D}[k]. \end{aligned} \tag{14}$$

The DFT property as stated by Eq. (14) and the discussions presented in this section provide both a powerful computational algorithm and appropriate interpretations of its output, as follows.

The sampled quadratic phase is a periodic signal when the sampling rate is chosen as stated before. The N-point DFT of one period of sampled quadratic phase gives the exact samples of the continuous Fourier transform of continuous quadratic phase within a constant gain factor. Periodic concatenations of the DFT output remain as exact samples of the continuous Fourier transform of the original continuous quadratic phase function. And these are true despite the fact that there is significant aliasing during sampling. This is not the case for arbitrary functions: usually, as a consequence of aliasing, the DFT of the input samples are not necessarily the exact samples of the continuous Fourier transform of the original continuous input function. In general, typical signal processing applications, the initial discretization related issues (aliasing etc.) and the issues related to simple utilization of DFTs to implement convolutions (i.e., circular convolution instead of linear convolution) are known and taken into consideration to minimize their undesirable effects. However, as shown in this paper, and as a consequence of the preceding discussion, both the aliasing and the circular convolution issues are much easier to deal with when the kernel is the quadratic phase function.

Probably the most important observation as a consequence of the results provided in this section is the fact that, if a periodic input object consisting of equally spaced impulsive elements diffracts an incident plane wave, the resultant Fresnel diffraction patterns at some specific distances are also periodic and impulsive. One period of this periodic and impulsive Fresnel diffraction pattern is computed exactly by the algorithm $\mathrm{DFT}_N^{-1}\{\mathrm{DFT}_N[f[n]]\sqrt{jN}h^*_{\alpha D}[n]\}$, where the resultant array elements correspond to the weights of the impulses which form the diffraction pattern. If, for example, X is fixed, then those α's corresponding to $\alpha=(\pi/2rX^2)$, $r=1,...,\infty$, would generate the impulsive and periodic Fresnel diffraction patterns, with period NX, $N=2r$. To convert the parameter α to physical parameters, we note that $\alpha=\pi/(\lambda z)$, where λ is the wavelength and z is the distance between the object and the diffraction planes. Therefore, the distance for periodic impulsive Fresnel diffraction is $z=(2rX^2)/\lambda$, $r=1,...,\infty$.

Since the Fresnel diffraction is a linear shift-invariant operator (a convolution), one can extend the results already presented to better fit the physical cases. For example, the condition on impulses at the input mask can be relaxed by replacing them with their low-pass counterparts; this will then result in replacing the impulses at the output (diffraction pattern) with also their same low-pass filtered versions. The overall discussion, including the DFT operations and the exactness of the solutions under the presented conditions, are still valid; we just simply interpret the input and output arrays of the DFTs as the weights of the associated "low-pass filtered impulses," instead of the weights of the impulses in the original case. If the impulsive (discrete) periodic input function is obtained by sampling a continuous periodic input function at a rate above its own Nyquist rate, we can recover the original continuous input with no

loss from its samples by passing the samples through a proper low-pass filter. If this is the case, we can perform the same low-pass filtering operation to the samples of the diffraction pattern as computed using the DFTs as in the above paragraph, and get the exact Fresnel diffraction pattern corresponding to the continuous input. Again, for this to be correct, the above-mentioned restriction that relates the sampling interval, the period, and the distance between the planes must be satisfied.

By the way, the output of DFT of the discrete Fresnel kernel is known analytically as shown by Eq. (14), under the stated conditions, and therefore, there is no need for a DFT computation to find its numerical result.

Note that the discussions above follow from the particular choice of $c_{\alpha,2\pi n/X}=1$ which led to Eq. (10). Other choices are also possible, leading to different forms of periodicities of larger sizes. For example, one can specify $c_{\alpha,2\pi n/X}=(-1)^n$. Following similar steps, we can compute the exact Fresnel diffraction pattern of a periodic and impulsive input whose one period is the pattern obtained by concatenating the discrete object (size N), with the same object pattern multiplied by -1. Thus the period becomes $2N$. The associated size-$2N$ discrete kernel, and its $2N$-point DFT, are $\exp[j(\pi/2N)n^2]$, and, $\sqrt{j2N}\exp[j(\pi/2N)k^2]$, respectively. Extensions to $c_{\alpha,2\pi n/X}=\{\exp[-j(2\pi/M)]\}^n$ will lead to M concatenations of the size-N object, where each concatenation multiplied by a complex number (M roots of 1); the kernel, and its DFT will be $\exp[j(\pi/MN)n^2]$ and $\sqrt{jMN}\exp[-j(\pi/MN)k^2]$, respectively. As expected, the obtained array elements correspond to the weights of the impulses of the periodic and impulsive exact Fresnel diffraction pattern for such objects at specified distances.

3 Extension to Two Dimensions

Naturally, simulations of optical phenomena will involve 2-D inputs and outputs. The extension of the properties discussed in the previous section is straightforward; therefore, we will not derive them, again. Instead, we will present the results corresponding to Eqs. (9) to (14) and then extend the discussions to interpret the 2-D DFT usage for Fresnel diffraction simulations.

Let $\mathbf{V}$ be the 2-D sampling matrix; therefore, sampling of a 2-D function $f(\mathbf{x})$, where $\mathbf{x}=[x\ y]^T$, is achieved by multiplying the function with a 2-D impulse mesh as, $f(\mathbf{x})\Sigma_{\mathbf{n}}\delta(\mathbf{x}-\mathbf{Vn})$. As usual, $\mathbf{n}=[n_1\ n_2]^T$. Matrix $\mathbf{U}$ is defined as $2\pi\mathbf{V}^{-T}$. Following similar steps as in the previous section, we get,

$$
\begin{aligned}
&f(\mathbf{x})**\left[h_\alpha(\mathbf{x})\sum_{\mathbf{n}}\ \delta(\mathbf{x}-\mathbf{Vn})\right]\\
&\quad=f(\mathbf{x})**\left[\sum_{\mathbf{n}}\ \left(\frac{1}{|\det\mathbf{V}|}c_{\alpha,\mathbf{Un}}\right)\delta\left(\mathbf{x}+\frac{\mathbf{Un}}{2\alpha}\right)\right]**h_\alpha(\mathbf{x})\\
&\quad=\left[\sum_{\mathbf{n}}\ \left(\frac{1}{|\det\mathbf{V}|}c_{\alpha,\mathbf{Un}}\right)f\left(\mathbf{x}+\frac{\mathbf{Un}}{2\alpha}\right)\right]**h_\alpha(\mathbf{x}),
\end{aligned}
\tag{15}
$$

where $**$ is now the 2-D convolution operation, and $c_{\alpha,\mathbf{U}_0}$ for a matrix index is $\exp[-j(\mathbf{U}_0^T\mathbf{U}_0)/4\alpha]$. If we choose to restrict the sampling matrix $\mathbf{V}$ to get $c_{\alpha,\mathbf{Un}}=1$ for all $\mathbf{n}$, then we can write

$$
\mathcal{F}\left[h_\alpha(\mathbf{x})\sum_{\mathbf{n}}\ \delta(\mathbf{x}-\mathbf{Vn})\right]=4\alpha^2H_\alpha(\mathbf{u})\sum_{\mathbf{n}}\ \delta(\mathbf{u}-2\alpha\mathbf{Vn}),
\tag{16}
$$

where the 2-D Fourier transform is from $\mathbf{x}$ domain to $\mathbf{u}$ domain. The restriction on the sampling matrix $\mathbf{V}$ to achieve above result is to satisfy that $(\pi/\alpha)\mathbf{V}^{-1}\mathbf{V}^{-T}$ is an integer matrix $\mathbf{P}$, and $\mathbf{q}^T\mathbf{Pq}$ is an even number for any integer array $\mathbf{q}$.

The impulsive nature of the right-hand side of preceding equation implies a 2-D periodicity of the left-hand side, where the associated 2×2 discrete domain periodicity matrix is $\mathbf{P}=(\pi/\alpha)\mathbf{V}^{-1}\mathbf{V}^{-T}$. [The corresponding continuous domain periodicity is described by the matrix $\mathbf{VP}=(\pi/\alpha)\mathbf{V}^{-T}$.] Indeed, this can also be shown directly, since,

$$
\begin{aligned}
h_{\alpha D}[\mathbf{n}]&\triangleq h_\alpha(\mathbf{Vn})=\exp[j\alpha(\mathbf{n}^T\mathbf{V}^T\mathbf{Vn})]\\
&=\exp\{j\alpha[(\mathbf{n}+\mathbf{Pq})^T\mathbf{V}^T\mathbf{V}(\mathbf{n}+\mathbf{Pq})]\}\\
&=h_\alpha[\mathbf{V}(\mathbf{n}+\mathbf{Pq})]=h_{\alpha D}[\mathbf{n}+\mathbf{Pq}]\quad\forall\mathbf{n},\mathbf{q},
\end{aligned}
\tag{17}
$$

where $\mathbf{q}$ is a 2-D vector with integer elements, and $\mathbf{P}$ satisfies the abovementioned relation.

Denoting the discrete array $h_{\alpha D}[\mathbf{n}]=h_\alpha(\mathbf{Vn})$, and $H_{\alpha D}[\mathbf{k}]=H_\alpha(2\alpha\mathbf{Vk})$ we further get

$$
\mathrm{DFT}_{\mathbf{P}}[h_{\alpha D}[\mathbf{n}]]\triangleq\sum_{\mathbf{n}=0}^{N-1}h_{\alpha D}[\mathbf{n}]\exp(-j2\pi\mathbf{k}^T\mathbf{P}^{-1}\mathbf{n}),
\tag{18}
$$

which turns to

$$
\begin{aligned}
&\mathrm{DFT}_{N\times N}[h_{\alpha D}[\mathbf{n}]]\\
&\quad\triangleq\sum_{\mathbf{n}=0}^{N-1}h_{\alpha D}[\mathbf{n}]\exp\left(-j\frac{2\pi}{N}\mathbf{k}^T\mathbf{n}\right)\\
&\quad=\frac{1}{|\det\mathbf{V}|}H_{\alpha D}[\mathbf{k}]=jNh^*_{\alpha D}[\mathbf{k}]\quad\text{for}\quad\mathbf{P}=\begin{bmatrix}N&0\\0&N\end{bmatrix}.
\end{aligned}
\tag{19}
$$

Thus, we obtain the desired tools to form and interpret the digital simulations to compute the Fresnel diffraction. As indicated in the previous section, if the input mask is periodic and consists of regularly spaced impulses, then the elements of the resultant array of $\mathrm{DFT}^{-1}_{N\times N}\{\mathrm{DFT}_{N\times N}(f[\mathbf{n}])\cdot jNh^*_{\alpha D}[\mathbf{k}]\}$ correspond to the weights of the periodic Fresnel diffraction pattern which also consists of regularly spaced impulses. The described diffraction pattern is not a numerical approximation, but an exact solution in the sense that if the described mask is placed in front of an incident wave and the continuous Fresnel diffraction is found, it will be the same as the described function. However, the restriction on the relations

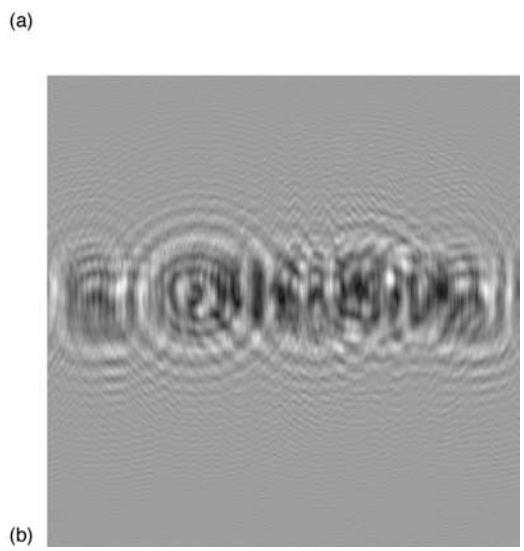

Fig. 1 Fast computation of exact Fresnel diffraction pattern using a DFT-based algorithm: (a) one period of a periodic mask, consisting of 256×256 square pixels, and (b) one period of its periodic exact Fresnel diffraction pattern, which also consists of 256×256 square pixels.

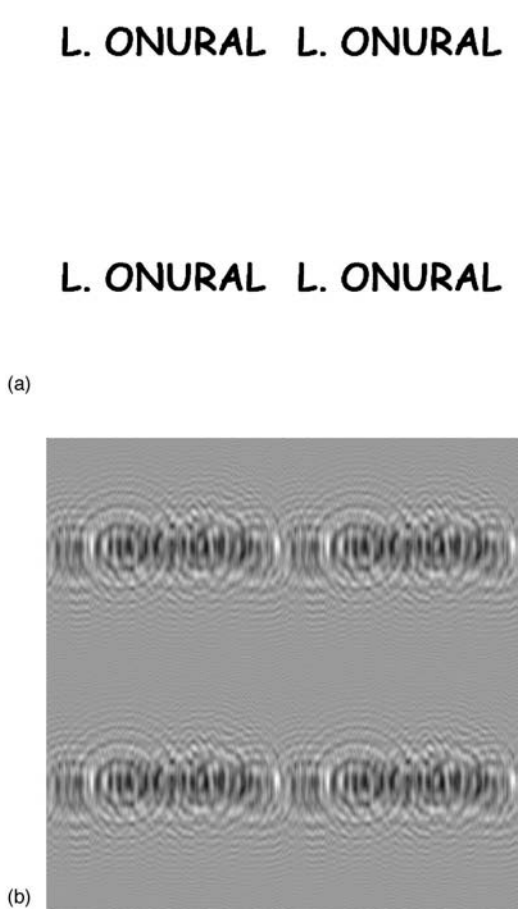

Fig. 2 Implied rectangular periodicity of the simulations shown in Fig. 1: (a) four periods of a periodic input mask, where each period consists of 256×256 square pixels and (b) the corresponding periodic exact Fresnel diffraction pattern, which also consists of square pixels.

between the sampling interval, pattern period, and the distance between the object and diffraction planes must obey the given constraint.

Following observations similar to those in the 1-D case, we know that we can apply the same linear operator to the input and the output and still keep the exact nature of the Fresnel diffraction relationship. A useful case is to convolve the input impulses by

$$h_f(\mathbf{x}) = \begin{cases} 1 & \mathbf{x} \in [0,X] \times [0,X] \\ 0 & \text{else.} \end{cases}$$

This is equivalent to converting each impulse to constant gray-level pixel for an input mask, which consists of pixels (mosaic). Using arguments similar to those in previous paragraph, we can get the corresponding exact Fresnel diffraction simply by implementing the given DFT-based algorithm, and then generating an image at the output, consisting of square pixels where each pixel value is equal to the corresponding element of the output array obtained from the algorithm. Please note that all this is possible as a consequence of the properties of the Fresnel kernel under sampling; approximation of a general convolution by DFTs would not normally lead to such a surprising result.

A 2-D example is shown in Fig. 1, where Fig. 1(a) is a 256×256 discrete object (transparent background, opaque letters *L. ONURAL*). Each discrete element is depicted as a square pixel with a uniform gray level. The periodicity matrix $\mathbf{P}=[\mathbf{p}_1\ \mathbf{p}_2]$, where $\mathbf{p}_1$ and $\mathbf{p}_2$ are equal to $[256\ 0]^T$ and $[0\ 256]^T$, respectively. So the corresponding sampling matrix is, $\mathbf{V}=[\mathbf{v}_1\ \mathbf{v}_2]$, where $\mathbf{v}_1$ and $\mathbf{v}_2$ are equal to $[(\pi/256\alpha)^{1/2}\ 0]^T$ and $[0\ (\pi/256\alpha)^{1/2}]^T$, respectively. Therefore, the example is for the simple rectangular sampling case.

The circular convolution kernel is $h_{\alpha D}[\mathbf{n}]=h_\alpha(\mathbf{Vn})=\exp[j\alpha(\mathbf{n}^T\mathbf{V}^T\mathbf{Vn})]=\exp[j(\pi/256)\mathbf{n}^T\mathbf{n}]$ for n_1, $n_2 \in [0,255]$. The DFT of this function is known analytically as $jN\exp[-j(\pi/256)\mathbf{k}^T\mathbf{k}]$. Figure 1(b) shows the magnitude of the complex pattern $\mathrm{DFT}^{-1}\{\mathrm{DFT}[f[n]] \cdot jN\exp[-j(\pi/256)\mathbf{k}^T\mathbf{k}]\}$, where each array element is depicted as a square pixel, exactly as done for the input array.

Therefore, the diffraction pattern of Fig. 1(b) is the exact Fresnel diffraction pattern in magnitude of the periodic input whose one period is shown in Fig. 1(a). In other words, if a periodic pattern whose four periods are shown in Fig. 2(a) is physically brought in front of an incident plane wave, and if the Fresnel approximation is valid, the magnitude of the optical diffraction pattern at the corresponding distance will be exactly like the periodic pattern shown in Fig. 2(b). The corresponding sampling interval X is $(\lambda z/256)^{1/2}$, and the period of the input and Fresnel diffraction patterns is $256X \times 256X$. We can convert the normalized parameters to physical counterparts by noting that $(NX^2/\lambda z)=1$. Therefore, if $\lambda=0.6\ \mu$m, and $X=100\ \mu$m, the simulation of Fig. 1(b) corresponds to the Fresnel diffraction at $z=4.26$ m; both the mask and its diffraction patterns are periodic in both directions with a period of 25.6 mm with square tile geometry. The same simulation result correspond to many different physical cases, as long as X, λ, and z satisfy the preceding condition.

Incidentally, the discrete kernel $\exp[j(\pi/N)\mathbf{n}^T\mathbf{n}]$ is also the kernel which is used in simulations in Ref. 3.

4 Conclusions

Sampling of the quadratic phase function causes aliasing since this function is not bandlimited. The form of aliasing, however, is very specific and manageable. A sampled version of the quadratic phase function is equal to shifted and overlapped continuous quadratic phase functions. The Fourier transform of the sampled quadratic phase function is equal to (within a constant gain factor) samples of its own complex conjugate if some conditions are imposed on the sampling interval. A sampled quadratic phase function can be a periodic signal for some sampling rates; unlike the general case for arbitrary functions, the DFT of one period of the quadratic phase function is equal to (within a constant) exact samples of the continuous Fourier transform of the original continuous quadratic phase function, despite the fact that there is aliasing. These results are important when discretization of diffraction related signals is needed for digital computation.

Looking at the discussions, it is interesting to see that some operations on the quadratic phase function in the space domain results in similar types of operations in the Fourier domain. For example, a shift in space results in a shift in the Fourier domain; similarly, a modulation also transforms to a modulation. Some of these are well known and utilized in practice: for example, the real part of the quadratic phase function has been used to test the frequency response of imaging and image transmission (TV) systems for many decades since the frequency response can be seen from the space attenuation distribution of the quadratic phase function. However, the extent of such invariance is interesting to investigate: for example, as proven in this paper, sampling in the space corresponds to sampling in the Fourier domain. The primary reason behind this invariance of the operations in the space and Fourier domains can be attributed to the fact that the quadratic phase function has a linearly increasing instantaneous frequency.

Using these properties it is shown that exact Fresnel diffraction patterns of periodic masks at certain distances can be efficiently computed using DFTs. Furthermore, we also conclude that the exact Fresnel diffraction patterns of a periodic mask consisting of regularly spaced impulses are also periodic and consist of regularly spaced impulses for some distances.

The provided results are important in designing digital diffraction simulators and interpreting the outputs of such simulators appropriately.

Furthermore, the DFT relations given in this paper also form an efficient recipe to compute the discrete fractional Fourier transform for some values of the fraction.

References

1. J. W. Goodman, *Introduction to Fourier Optics*, 2nd ed., Chap. 4, McGraw-Hill, New York (1996).
2. G. A. Tyler and B. J. Thompson, "Fraunhofer holography applied to particle size analysis: a reassessment," *Opt. Acta* **23**(9), 685–700 (1976).
3. L. Onural and P. D. Scott, "Digital Decoding of In-line Holograms," *Opt. Eng.* **26**(11), 1124–1132 (1987).
4. H. M. Ozaktas, M. A. Kutay, and D. Mendlovic, "Introduction to the fractional Fourier transform and its applications," Chap. 4 in *Advances in Imaging and Electron Physics*, Vol. 106, P. W. Hawkes, Ed., pp. 239–291, Academic Press, San Diego, CA (1999).
5. X. Deng, B. Bihari, J. Gan, F. Zhao, and R. T. Chen, "Fast algorithm for chirp transforms with zooming-in ability and its applications," *J. Opt. Soc. Am. A* **17**(4), 762–771 (2000).
6. A. J. Lambert and D. Fraser, "Linear systems approach to simulation of optical diffraction," *Appl. Opt.* **37**(34), 7933–7939 (1998).
7. M. Cywiak, M. Servin, and F. M. Santoyo, "Wavefront propagation by Gaussian superposition," *Opt. Commun.* **195**(5–6), 351–359 (2001).
8. L. Onural, "Sampling of the diffraction field," *Appl. Opt.* **39**(32), 5929–5935 (2000).
9. L. Yu, Y. An, and L. Cai, "Numerical reconstruction of digital holograms with variable viewing angles," *Opt. Express* **10**(22), 1250–1257 (2002).
10. M. J. Simpson, "Diffraction pattern sampling using a holographic optical element in an imaging configuration," *Appl. Opt.* **26**(9), 1786–1791 (1987).
11. T. M. Kreis, "Frequency analysis of digital holography with reconstruction by convolution," *Opt. Eng.* **41**(4), 771–778 (2002).
12. H. M. Ozaktas, O. Arikan, M. A. Kutay, and G. Bozdağı, "Digital computation of the fractional Fourier transform," *IEEE Trans. Signal Process.* **44**, 2141–2150 (1996).
13. S. Coetmellec, D. Lebrun, and C. Özkul, "Application of the two-dimensional fractional-order Fourier transformation to particle field digital holography," *J. Opt. Soc. Am. A* **19**(8), 1537–1546 (2002).
14. D. Lebrun, A. M. Benkouider, S. Coetmellec, and M. Malek, "Particle field digital holographic reconstruction in arbitrary tilted planes," *Opt. Express* **11**(3), 224–229 (2003).
15. U. Schnars and W. P. O. Jüptner, "Digital recording and numerical reconstruction of holograms," *Meas. Sci. Technol.* **13**(9), R85–101 (2002).

Levent Onural received his PhD degree in electrical and computer engineering from State University of New York at Buffalo in 1985 and his BS and MS degrees are from Middle East Technical University in 1979 and 1981, respectively. He was a Fulbright scholar between 1981 and 1985. After being a research assistant professor with the Electrical and Computer Engineering Department of the State University of New York at Buffalo, he joined the Electrical and Electronics Engineering Department of Bilkent University, Ankara, Turkey, where he is currently a full professor. His current research interests are image and video processing, with an emphasis on video coding, holographic TV, and the signal processing aspects of optical wave propagation. Dr. Onural received an award from TÜBITAK of Turkey in 1995 and a Third Millenium Medal from IEEE in 2000. He directed the IEEE Region 8 (Europe, Middle East, and Africa) in 2001 to 2002, was the Secretary of the IEEE in 2003, and was a member of the IEEE Board of Directors in 2001 to 2003, the IEEE Executive Committee in 2003, and the IEEE assembly in 2001 to 2002. He is currently an associate editor of *IEEE Transactions on Circuits and Systems for Video Technology*.